

Geochemical speciation of iron under nearshore hypoxia: A case study of Alappuzha mud banks, southwest coast of India

Mathew^a, D., Gireeshkumar, T. R^{*a}., Udayakrishnan, P.B^b., Shameem, K^c., Nayana, P.M^a., Deepulal, P.M., Sarath, R., Nair, M^a., Jaleel, A.K.U^a., Balachandran, K.K^a

^aCSIR - National Institute of Oceanography, Regional Centre, Kochi - 682 018, India
Phone: +914842390814, Fax: +914842390618

^bCSIR - National Institute of Oceanography, Regional Centre, Mumbai - 400 053, India
Phone: +912226359605, Fax: +912226364627

^cInter University Centre for Development of Marine Biotechnology
School of Marine Sciences, Cochin University of Science and Technology. Kochi-682016

*Corresponding author's E-mail address: gkumar@nio.org

Abstract

Studies on the speciation of iron (Fe) and its regulatory roles in the biogeochemical cycling of other elements in the sediments of the Arabian Sea are limited. Changes in the reactivity and crystallinity of geochemical forms of Fe were determined in the Alappuzha mud bank on the southwest coast of India, which experiences hypoxia during the southwest monsoon. Fortnightly time-series measurements were conducted from April to August 2016. Coastal upwelling was evident from June onwards and caused hypoxic water's incursion until August. The mud bank sediments are geochemically unique due to high concentrations of Fe, phosphorus (P) and moderate levels of organic matter, nitrogen (N), and sulfur (S). Geochemical speciation of Fe showed significant concentrations of easily reducible Fe oxides (Fe_{OX1}), reducible crystalline Fe oxides (Fe_{OX2}), sheet silicate bound Fe (Fe_{PRS}), unreactive Fe (Fe_U), magnetite (Fe_{MAG}), and pyrite-bound Fe (Fe_{PYR}). The concentrations of total Fe (Fe_T) and highly reactive Fe (Fe_{HR}) in mud bank sediments were 63.5 and 37 mg/g, respectively, much higher than those in other coastal sediments, including upwelling zones. Fe_T remained in the sediments even under hypoxia, in contrast to the pronounced Mn decrease, indicating Mn mobilization from surface sediments. Various Fe ratios/indices such as Fe_{PYR}/Fe_{HR}, and Fe_{HR}/Fe_T revealed anoxic and ferruginous conditions in the sediments during upwelling. Highly reactive Fe(III) oxides (Fe_{OX1} and Fe_{OX2}) were the primary Fe pool in the mud bank sediments, and they effectively immobilized the free sulfide formed by sulfate reduction. The high sulfide buffering capacity is significant for the environment as it can rapidly immobilize the dissolved sulfide, a potent toxin for benthic and demersal organisms.

Keywords: Iron; Speciation; Upwelling; Hypoxia; Clay

1. Introduction

Redox cycling of Fe profoundly influences the geochemical cycling of elements such as carbon (C), S, and P as well as various trace metals in the marine environment (Burdige, 1993; Otero et al., 2010; Taylor and Konhauser, 2011; Zhu et al., 2015). In oxygenated marine sediments, Fe exists as Fe (III) oxides, hydroxides, and oxy-hydroxides (hereafter Fe (III) oxides) with various chemical compositions, minerals and crystal structures. Fe (III) oxides effectively immobilize phosphates and several transition elements in sediments (Burdige, 1993; Hyacinthe and Van Cappellen, 2004; Zhu et al., 2012). Fe (III) oxides exhibit different reactivities towards biotic and abiotic reduction depending on their geochemical characteristics (Canfield et al., 1989; Canfield, 1992; Thamdrup, 2000; Hyacinthe et al., 2006; Zhu et al., 2015). Reactive Fe oxides act as terminal electron acceptors after the depletion of other thermodynamically favourable electron acceptors, such as oxygen (O₂), nitrate (NO₃⁻), and Mn (IV) oxides (Froelich et al., 1979). Under suboxic conditions, enrichment of Fe(III) oxides combined with low or moderate labile organic matter inhibits sulfate reduction. Fe(III) oxide reduction leads to anaerobic oxidation of organic matter (Vandieken et al., 2006; Nickel et al., 2008). The resulting Fe(II) either forms Fe_{pyr} with available bisulfide (HS⁻) in the anoxic layer of the sediment (Jørgensen, 1977; Chanton et al., 1987) or re-oxidizes in the oxic layer of the sediment or water column (Zhu et al., 2012).

The domain for this study is the Alappuzha mud bank that offers a unique environment during the southwest monsoon at the southwest coast of India (Jyothibabu et al., 2018). The persistent mud bank is different from other major mud banks/muddy coasts around the world (Kurup, 1977; Wells and Coleman, 1981; Aller, 1998; Walsh and Nittrouer, 2004; Liu et al., 2006; McBride et al., 2007; Anthony et al., 2008) due to its remoteness from riverine sources. Mud banks form as a fluid mud layer at the bottom of the sea, progressively attenuating high waves and facilitating a calm coastal environment during the turbulent monsoon (Shynu et al., 2017; Gireeshkumar et al., 2020). Tranquil waters have significant socio-economic implications as they provide platforms for local fishing and protect beaches throughout the rough monsoon.

In the past decades, studies on the Alappuzha mud banks have resulted in several hypotheses explaining the formation of mud banks (Bristow, 1938; Kurup, 1972; Nair, 1976; CMFRI Bulletin 1984; Mathew and Baba, 1995; Tatavarti et al. 1996, and 1999; Mallik et al., 1998; Mathew and Gopinathan, 2000; Balachandran et al., 2004; Narayana et al., 2008; Dinesh and Jayapraksh, 2008; Muraleedharan et al., 2017; Badesab et al., 2018; Gireeshkumar et al., 2020). The formation of mud banks is generally attributed to different force mechanisms such as winds, waves, currents, wave-mud interaction, upwelling, deformation, subterranean mud and freshwater flow. Sediment properties could

also be significant (Nair, 1976; Murty et al., 1984; Ramachandran and Samsuddin, 1991) because the mud banks are formed as a fluid mud layer close to the bottom of the sea (Mallik et al., 1988; Shynu et al., 2017). Montmorillonite, the dominant clay mineral in the fluid mud, geochemically interact with oxyanions (phosphates) to make mud banks stable and sustainable (Gireeshkumar et al., 2020).

The southwest coast of India experiences basin-wide coastal upwelling during southwest monsoon (Naqvi et al., 2000; Gupta et al., 2016), and the Alappuzha mud banks co-exist with the upwelling phenomenon. The incursion of cold, nutrient-replete, oxygen-deficient subsurface waters towards the coast leads to significant plankton growth, indicating coastal upwelling (Madhupratap et al., 2001; Jagadeesan et al., 2017). During upwelling, hypoxic waters were intruded to shallow depths (< 3 m) of the Alappuzha mud bank (Gireeshkumar et al., 2017; Mathew et al., 2019). Predicted metabolic activities of the microbes in the water column during hypoxia include dehalogenation, sulfate and nitrate reductions, and ammonia oxidation (Anas et al., 2018; Parvathi et al., 2019). The variations in the dissolved oxygen levels can significantly vary the geochemical partitioning of biogenic elements, including Fe, in mud banks. Further, the redox cycling of Fe may play a significant role in its supply to the overlying water column to support primary productivity.

Not many studies have been conducted around the distribution, speciation, and transformation of Fe forms under varying oxygen conditions in nearshore waters (depth <13 m). This study is based on the time-series observations during April - August 2016 of three shallow locations (depth <13 m) in and around the Alappuzha mud banks. The study delineates the geochemical variations of Fe in undulating oxic and hypoxic environments. A mud bank is characterized by high mud content, dynamic fluidized surface mud and increased biological productivity/organic enrichment induced by upwelling. Thus, it provides an excellent opportunity to trace the distribution of Fe pools in coastal regions. In this study, we explore the response of various Fe forms to the changes in and around the mud bank during upwelling.

2. Material and Methods

2.1. Time-series Sampling

As shown in Fig. 1, we selected three stations (M1, M2 and M3) in and around the Alappuzha mud bank for sampling during April to August 2016, covering monsoon and non-monsoon periods. M1 (7 m water depth) was a non-mud bank region, while M2 (7 m water depth), located 7 km south of M1, represented the Alappuzha mud banks. M3 (13 m water depth) was an offshore point to the west of M2. Salinity and temperature were recorded with accuracies of ± 0.001 and ± 0.0001 , respectively, using the SBE 19 plus conductivity, depth and temperature (CTD) profiler. For dissolved

oxygen (DO) and nutrients, water samples were collected using a 5L Niskin water sampler. Sediments were collected using a Van Veen grab (0.04 m²). Though box and multiple corers are suitable for collecting undisturbed sediment samples, Van Veen grabs can be used with caution for this type of study. Several deployments per station were carried out to collect well-preserved sediment samples to avoid bias due to the washout of supernatant water and possible disturbance of the surface sediment during the grab operation. The 1-2 cm surface layer was skimmed off using a pre-cleaned scoop and stored in clean high-density polyethylene (HDPE) bottles in an inert atmosphere at 4°C till analysis.

2.2. Laboratory Methods

Dissolved oxygen was estimated following the Winkler method (Grasshoff et al., 1983) using an automated titration system (Metrohm 865 Dosimat plus; detection limit 2µM). Sediment texture was determined using pipette analysis (Folk, 1980), after removing carbonates and organic matter from wet sediment using 1M hydrochloric acid (HCl) and 30% hydrogen peroxide (H₂O₂), respectively. Vacuum dried samples were powdered with a mortar and pestle for elemental analysis. For total organic carbon (TOC) analysis, sediments were pre-treated with 1M HCl to remove carbonates, washed with deionized water to remove salts, and freeze-dried. TOC, total nitrogen (TN), and total sulfur (TS) were determined using a Vario EL III CHNS analyzer with detection limits of 0.07%, 0.01%, and 0.01% for TOC, TN, and TS, respectively. Sediments were digested in the Milestone Ethos Easy microwave digester using a 7:3:1 mixture of nitric acid (HNO₃), HCl, and hydrofluoric (HF), and analyzed for Fe and Mn using an inductively coupled plasma-optical emission spectrophotometer (Thermo Scientific i-CAP 7000 Series). The lower detection limits were 12.50 for Fe and 3.50 µg/g for Mn. Another set of sediment samples was then open digested on a hot plate using a mixture of perchloric acid (HClO₄), HNO₃, and HCl. The extract was analyzed for total P using the Skalar SAN⁺⁺ auto-analyzer and the standard procedure proposed by Grasshoff et al. (1983).

2.3. Fe Speciation

Fe speciation was conducted using wet sediment samples with a stepwise chemical extraction procedure in an inert environment. Poulton and Canfield (2005) modified the sequential extraction procedure proposed by Tessier et al. (1979) and Poulton and Raiswell (2002). We adopted the new procedure for this study as it identifies magnetite and Fe carbonates separately, as shown in Fig. 2. The efficacy of the extraction and the solubility of sedimentary Fe minerals may vary based on the grain size, crystallinity, and complex association of minerals with the sediment matrix (Slotznick et al., 2020).

In the sequential extraction procedure, Fe_{Carb} fraction (siderite and ankerite) was extracted from wet sediment in 48 h using sodium acetate (NaCH₃COO) maintained at 4.5 pH and 50°C. Buffered sodium acetate at a pH of 4.5 is also extracted Fe bound to acid volatile sulfur. Fe_{Ox1} (ferrihydrite and lepidocrocite), Fe_{Ox2} (goethite, akageneite, and hematite), and Fe_{Mag} (magnetite) were extracted using hydroxylamine HCl, dithionite, and ammonium oxalate (C₂H₈N₂O₄), respectively. The three extractions were completed in 48, 2, and 6 h, respectively. Poorly reactive (silicate) Fe was separated from the residue by boiling it in 12 N HCl. A different sediment sample was dry ashed for 8 h at 450°C and subsequently boiled in 6 N HCl for 24 h to extract Fe_T. Fe_{Pyr} was separately extracted from wet sediment using the chromous-chloride distillation method, assuming chromium-reducible sulfur was pyrite (Canfield et al., 1986). Hydrogen sulfide (H₂S) was trapped as zinc sulfide (ZnS) in a vessel containing 3% zinc acetate (ZnC₄H₆O₄) and 10% ammonium hydroxide (NH₄OH) solution during distillation. Fe_{Pyr} concentration was estimated by iodometric titration using the Metrohm automatic titration system, and the relative standard deviations obtained from repeated analyses were <5%. Fe_U concentration was calculated by subtracting the sum of Fe_{Pyr} concentration and the first five fractions from Fe_T. Different Fe form's concentration was measured using atomic absorption spectrophotometer (Thermo scientific iCE 3000 series). All Fe forms were extracted thrice, and average concentrations were calculated. The triplicate analyses yielded a relative standard deviation of <6% for all extractions. As shown in Fig. 2, the Fe fractions were sub-divided into highly reactive (Fe_{HR}), poorly reactive (Fe_{PR}), and unreactive (Fe_U) pools based on their reactivity determined under standard protocols (Poulton and Canfield, 2005). Fe_{HR} concentration was calculated by adding the concentrations of Fe_{Pyr}, Fe_{Mag}, and Fe_{Carb} to those of Fe(III) oxides Fe_{Ox1} and Fe_{Ox2}, assuming Fe(II) forms are reduced Fe(III) oxides (Poulton and Canfield, 2005). The sum of concentrations of Fe_{Ox1} and Fe_{Ox2} gives the Fe(III)_{HR} concentration. Fe(III)_{HR} oxides readily react with sulfides and provide the buffering capacity in marine sediments (Zhu et al., 2012). Triplicate extractions were carried out, and the average values were reported.

3. Results

3.1 General Hydrography

The study region remained warm and vertically mixed during April - May (30-32°C) and started cooling gradually during June-September to 23-26°C due to monsoon-induced upwelling. As shown in Fig.3, salinity did not vary widely, except for a few low saline patches, due to erroneous values recorded by the CTD when in contact with the fluid mud layer (Muraleedharan et al., 2017a). At M3, DO levels decreased sharply due to prolonged upwelling during 14 June–31 August; however, the intrusions of upwelled water at M1 and M2 were intermittent during 14 June–10 August. The DO

concentrations in the sub-surface waters fell below 60 μM in both M1 (52 μM) and M3 (42 μM) at the onset of the southwest monsoon below the well-oxygenated surface waters layer. The temperature of the water column (from <2 m to the bottom), overlain by a thin, warm, low salinity lens in the nearshore region, decreased to <26°C, its salinity rose to >35.5 PSU, and it became oxygen-deficient with DO concentration <65 μM due to upwelling (Gireeshkumar et al., 2017; Mathew et al., 2019). Heavy rainfall during southwest monsoon results in stratification in the upper layer, which curtails vertical mixing and helps maintain a two-layered structure in the nearshore region despite strong winds (Prasanna Kumar et al., 2018).

3.2 Bulk Geochemistry

The sediment was predominantly clay or silty clay (Fig. 4). The sediment had a moderate concentration of bulk elements such as TOC (2.42 ± 2.85 %), TN (0.27 ± 0.41 %) and TS (1.04 ± 1.30 %) (Fig. 5). Pearson correlation analysis was performed using SPSS, and TS and TOC showed a significant positive correlation with a p -value <0.01. As shown in Table 1, mean Mn concentrations were 107.57 ± 28 $\mu\text{g/g}$, 102 ± 21 $\mu\text{g/g}$, and 102.63 ± 25 $\mu\text{g/g}$ at M1, M2 and M3, respectively, showing a decreasing trend with intensifying of upwelling.

3.3 Total Fe and Fe Speciation

As shown in Fig. 6, Fe_T concentrations in the sediments were 58.34–66.99 mg/g, 56.06–74.34 mg/g, and 53.34–66.60 mg/g at M1, M2, and M3, respectively. Fig. 6a shows low Fe_{Carb} , contributing <1% to Fe_T . Fe_{Ox1} gradually increased during upwelling, contributing 19%–37.3%. In contrast, Fe_{Ox2} decreased during hypoxia, accounting for 14.5%–26.7%. Fe_{Mag} also notably decreased (<10%) during hypoxia. Fe_{PRS} was 17.5%–37% and Fe_{Pyr} contributed <8%. Fe_U decreased sharply, from mid-June onwards, at all the stations. Fe_{HR} accounted for 34.26 ± 2.12 , 36.96 ± 2.17 , and 37.66 ± 1.10 mg/g at M1, M2, and M3, respectively. As shown in Table 1, $\text{Fe}_{\text{HR}}/\text{Fe}_T$ and $\text{Fe}_{\text{Pyr}}/\text{Fe}_{\text{HR}}$ ratios were 0.50 ± 0.04 and 0.10 ± 0.02 , 0.52 ± 0.06 and 0.08 ± 0.02 , and 0.56 ± 0.05 and 0.07 ± 0.01 for M1, M2, and M3, respectively.

4. Discussion

Mud bank sediments are mostly clay or silty-clay (Nair et al., 1966 and 1976; Dora et al., 1968; Kurup, 1977; Mallik and Ramachandran, 1984; Purandara and Dora, 1987) and composed of aluminosilicate clay minerals such as kaolinite, montmorillonite, and illite (Mathew, 1992; Mathew and Baba, 1995; Nath et al., 2000). In this study, we observed a sharp change in the sediment texture from silty-clay to clay soon after peak monsoon during July-August, with clay content increasing to > 80% (Fig. 4). Upwelling persisted in the study domain from June onwards, bringing hypoxic waters

(with $DO < 62 \mu M$) to depths < 3 m (Gireeshkumar et al., 2017; Mathew et al., 2019) and sustained for a longer period, especially at M3. The varying redox conditions at the sediment-water interface significantly influence sedimentary elemental speciation. During upwelling, mud bank sediments are rich in P (0.3 %) and moderate concentrations of organic matter, TN, and TS (Mathew et al., 2020).

The average concentration of Fe_T (6.35 ± 0.61 wt.%) in the Alappuzha mud bank is higher than those reported (≈ 3.5 wt.%) for other coastal margins (Slomp., 1996; Raiswell and Canfield, 1998; Clarkson et al., 2014; Li et al., 2016), and in range with concentrations reported earlier for the same region (Balachandran et al., 2003). The study region is at the coast of Kerala, bordered by the Western Ghats in the east and the Arabian Sea in the west. The flat-topped hills and ridges between the Western Ghats foothills and the Arabian Sea are formed of laterite. Hematite capping of magnetite bearing rocks is also prevalent in this region (Murthy, 1975; Mallik et al., 1987). All these Fe bearing forms may be significant contributors to the abundance of Fe in the mud bank sediments.

The concentrations of Fe_T and Mn in the sediments (Table 1) decrease with depletion of oxygen in the water column, with more reduction of Mn in the sediments compared to Fe. If the water column is well oxygenated, organic matter uses oxygen (as electron acceptor) in the sediment surface for oxidization. In the deeper layers, Mn^{4+} reduces to Mn^{2+} , which diffuses upward and gets re-oxidized at the oxic sediment surface (Froelich et al., 1979). However, during upwelling, hypoxia favours the reduction of Mn^{4+} to Mn^{2+} , which is released to the water column, leading to a decrease in Mn concentration in the surface sediments (Schulz et al., 2006). Fe(II) reprecipitates in the surface sediments even in mild oxygen deficiency (Krom and Berner, 1980; Jensen et al., 1995; Slomp et al., 1996).

As shown in Fig. 6b, concentrations of Fe pools, that is, Fe_{HR} (ferric oxides, carbonates, and sulfides), Fe_{PRS} (sheet silicate Fe), and Fe_U (residual silicate Fe) were calculated to quantify Fe partitioning and reactivity (Poulton and Raiswell, 2005; Li et al., 2016). The concentration of Fe_{HR} in mud banks (Canfield et al., 1992; Poulton et al., 2004) is more than that of Fe_{PRS} or Fe_U (Poulton and Raiswell, 2002).

Fe(III) oxides dominated in Fe_{HR} (Fe_{ox1} vs. Fe_{HR} , $p < 0.01$) with remarkably high $Fe(III)_{HR}/Fe_{HR}$ ratios of 0.78 ± 0.03 , 0.79 ± 0.01 and 0.80 ± 0.02 at M1, M2, and M3, respectively (Fig. 7b; Table 1), and Fe_{HR} decouples from Fe_T is in line with earlier reports (Raiswell and Canfield, 1998). Fe(III) mineral precipitation is the primary diagenetic process in the surface sediment during April-May, though the dissolution of Fe oxides, based on their reactivity is probably active underneath (Garrels and Christ, 1965; Pourbaix, 1974; Roberts, 2015).

As shown in Fig. 7a, Fe_{Ox1} and Fe_{Ox2} concentrations during 20 April-8 June indicated a steady-state in the study domain. Highly reactive Fe_{Ox1} declined slightly during 14-24 June, indicating the reductive dissolution of Fe oxides due to hypoxia followed by an unexpected Fe enrichment. The enrichment may be due to the re-oxidation of Fe^{2+} ions during the initial stage of oxide precipitation (Widdel et al., 1993; Dill et al., 1994; Laufer et al., 2016; Straub et al., 1996;). Low oxygenated waters may suppress the enrichment. In contrast, enrichment in the clay fraction suggests an abundance of Fe_{Ox1} particles, of size 10-20 nm, at the edges of aluminosilicates (Greenland and Mott, 1978) or as surface coatings (Poulton and Raiswell, 2005).

The decrease of Fe_{Ox2} levels from 10 July onwards, especially at M2, could be due to the goethite and hematite dissolution under more reducing conditions (Canfield, 1989), substantiated by its negative correlation with S ($p < 0.01$). Fe_{Ox1} and Fe_{Ox2} ($\text{Fe(III)}_{\text{HR}}$) are highly reactive to free sulfide, with a half-life period of days or weeks (Canfield et al., 1992; Raiswell and Canfield, 1998), and offer readily available buffering capacity to dissolved sulfides (Azzoni et al., 2005; Zhu et al., 2012). Buffering capacity effectively immobilizes free sulfides, which are potential toxins for benthic and demersal organisms, via precipitation of Fe(II) sulfides.

High concentrations of Fe_{HR} in mud bank sediments are due to the abundance of Fe oxides, and seasonal hypoxia enriches Fe oxides in the coastal surface sediments (Rozan et al., 2002; Sulu-Gambari et al., 2012, Hermans et al., 2019; Burdige and Komada, 2020). Formation of amorphous Fe oxides below the sediment-water interface due to remineralization of organic matter and oxidation of pore water Fe (II) or sedimentary Fe sulfides under hypoxia contribute to such an enrichment of Fe oxides (Burdige and Komada, 2020). Another case of Fe oxide enrichment is cable bacteria activity (Sulu-Gambari et al., 2012; Herman et al., 2019).

However, there are no reports on the distribution of cable bacteria either in mud banks or the southeastern Arabian Sea. Amorphous Fe oxides are highly reactive towards reductive dissolution and are thus, biologically accessible to phytoplankton through a variety of solubilization processes including photochemical Fe reduction and uptake by siderophores (Miller and Kester, 1994; Barbeau and Moffett, 2000; Kraemer et al., 2005; Kranzler et al., 2011; Basu and Shaked, 2018). A high load of suspended sediments indicates the resuspension of clay-sized particles at mud banks induced by strong winds and high waves associated with the southwest monsoon (Shynu et al., 2017; Prassanna Kumar et al., 2018). Such resuspensions may be a source of Fe in the shallow water column at mud banks.

As shown in Fig. 7a and b, the concentrations of Fe_{Mag} and Fe_{Pyr} in mud bank sediments are relatively low, while those of Fe_{Carb} are negligible. Fe_{Mag} exhibits variable reactivity depending on the source, mineralogy, and grain size distribution (Poulton and Raiswell, 2005; Zhu et al., 2012). Fine-grained Fe_{Mag} shows comparable reactivity to goethite and hematite (Fe_{Ox2}) (Poulton et al., 2004), substantiated by the temporal variations of Fe_{Mag} and Fe_{Ox2} in this study. The commencement of monsoon enriched Fe_{Mag} , followed by a decline from 10 July due to more reducing conditions in the sediment. The concentrations of Fe_{Mag} in the mud bank sediments were higher compared with those in other coastal sediments (Canfield and Berner, 1987; Lesli et al., 1990) even after considering the inherent errors in the magnetic separation methods (Lesli et al., 1990; Zhu et al., 2012), and maybe related to the geological evolution of this region, where hematite caps magnetite-bearing rocks (Mallik et al., 1987). Biologically induced (due to the attachment of Fe(II) to Fe(III) oxides) and biologically controlled (by magnetotactic bacteria) magnetite formations are also found in sediments ranging from Fe-rich suboxic to anoxic (Konhauser, 2006).

Enrichment of Fe_{HR} was observed in the study domain. Such enrichment is expected in hypoxic sediments due to rapid biological oxidation of Fe at seawater pH even under low oxygen conditions (Stumm and Morgan, 1981). Thus, Fe remains within sediments under aerobic and hypoxic conditions rather than moving to the overlying water column (Balzer, 1982).

The rate of pyrite formation is controlled by microbial sulfate reduction, depending on the buried organic carbon or the upward CH_4 flux and Fe availability (Goldhaber and Kaplan, 1974; Jorgensen, 1977, 1982, and 1990; Berner, 1984; Lyons, 1997; Raiswell and Canfield, 1998). The lower concentration of Fe_{Pyr} (0.23-0.45 wt%) is in line with the previously reported values (0.03-0.5 wt%) from the continental slope of the northern Arabian Sea and is due to low bottom water oxygen and high primary productivity (Morse, 1992; Schenau et al., 2002). Even though the Fe_{Carb} concentrations were low, it further decreased during hypoxia and increased later by August. Authigenic Fe(II) carbonates occur only in Fe-rich, non-sulfidic marine sediments (Canfield, 1989) and fluid mud layers in muddy coasts (Aller et al., 1988; Aller., 2004). The study region is characterized by the presence of a 0.2-1 m thick fluid mud layer close to the bottom of the sea (Shynu et al., 2017; Jyothibabu et al., 2018), and siderite ($FeCO_3$) is found at such fluidized sediment settings (Aller et al., 1988; Aller., 2004). Further studies based on mineralogy need to be conducted in the region to corroborate the observations.

The reactivity of Fe_{PRS} with sulfide is nearly 108 times lower than that of Fe (III) oxides, even after long exposure (Canfield et al., 1992). Fe-bearing sheet silicates (biotites, chlorites, illites, certain smectites) and Fe in montmorillonite are poorly reactive (Fe_{PRS}) (Raiswell et al., 1994) and other

fractions, derived from aluminosilicates, are unreactive (Fe_U) (Poulton and Raiswell, 2002). A decrease in Fe_U concentration soon after monsoon could be attributed to clay enrichment in the surface sediment. Fe_U exhibited a strong positive correlation with Fe_T ($r=0.78$, $p<0.01$), and it is in good agreement with the global marine sediments (Poulton and Canfield, 2005). In the study region, kaolinite (non-expandable), followed by montmorillonite (expandable), were dominant in sediments till the onset of monsoon; however, from mid June, very fine montmorillonite became abundant in surface sediments (Purandara, 1990; Mathew, 1992; Mathew and Baba, 1995; Gireeshkumar et al., 2020). Montmorillonite is rich in Fe (Slomp et al., 1996; Knebel et al., 1968; Hedges et al., 2003) and substantiates Fe_{PRS} enrichment in the region.

Different Fe_T contents and various relative fractions (due to carbonates and organic matter) in sediments globally make the comparison of Fe species in marine sediments difficult. Therefore, Fe-based indices, such as Fe_{HR}/Fe_T and Fe_{Pyr}/Fe_T , are calculated to infer Fe dynamics in marine sediments (Poulton and Raiswell, 2002). A widely utilized geochemical proxy to determine the environmental behaviour of Fe is the Fe_{HR}/Fe_T ratio (Raiswell and Canfield, 1998; Poulton and Raiswell, 2002; Lyons and Severmann, 2006; Poulton and Canfield, 2011). In general, Fe_{HR}/Fe_T ratios of marine sediments do not exceed 0.38 during deposition under oxic water conditions (Clarkson et al., 2014). The Fe_{HR}/Fe_T ratio in mud bank sediments was 0.43–0.49 when the water column was well oxygenated and increased gradually to 0.43–0.62 during hypoxia. These values were slightly higher than those calculated in previous studies for other oceanic regions. Ferruginous conditions can be determined from the extent of pyritization (Fe_{Pyr}/Fe_{HR}) of the highly reactive Fe pool in the euxinic state. The obtained ratio of 0.08 ± 0.02 confirmed ferruginous content in the study domain (März et al., 2008; Poulton et al., 2004; Poulton and Canfield, 2011; Clarkson et al., 2014).

5. Conclusions

In this study, we examined the changes in the Fe forms, their reactivity and sulfide buffering capacity in the seasonally hypoxic coastal environment of the Alappuzha mud bank on the southwest coast of India. Fe remained in the sediments even under hypoxic condition, while the reductive dissolution and subsequent release of Mn from sediments were evident. The Fe fractions in the mud bank showed unique features such as the dissolution of Fe(III) oxides and the slight enrichment of Fe_{Pyr} , possibly due to the reducing conditions in the sediments augmented by the fluid mud layer. $Fe(III)_{HR}$ was highly concentrated in the mud bank, providing a high buffering capacity to bind sulfide.

Acknowledgements

The authors thank the facilities and the support provided by the Director, National Institute of Oceanography and the Scientist in Charge, Regional Centre-Kochi. We appreciate the services rendered by our colleagues of CSIR-NIO in carrying out the field sampling successfully. We would like to thank the Ministry of Earth Sciences, Government of India, for financial support (Grant No. MoES/36/OOIS/Extra/22/2016). We sincerely thank the associate editor and two anonymous reviewers for the constructive and helpful comments. This is NIO contribution No. ...

References

- Aller, R. C., Heilbrun, C., Panzeca, C., Zhu, Z., Baltzer, F., 2004. Coupling between sedimentary dynamics, early diagenetic processes, and biogeochemical cycling in the Amazon-Guianas mobile mud belt: Coastal French Guiana. *Mar. Geol.* 208, 331–360. <https://doi.org/10.1016/j.margeo.2004.04.027>
- Aller, R. C., Rude, P. D., 1988. Complete oxidation of solid phase sulfides by manganese and bacteria in anoxic marine sediments. *Geochim. Cosmochim. Acta* 52, 751–765. [https://doi.org/10.1016/0016-7037\(88\)90335-3](https://doi.org/10.1016/0016-7037(88)90335-3)
- Anas, A., Sheeba, V. A., Jasmin, C., Gireeshkumar, T.R., Mathew, D., Krishna, K., Nair, S., Muraleedharan, K.R., Jayalakshmy, K. V., 2018. Upwelling induced changes in the abundance and community structure of archaea and bacteria in a recurring mud bank along the southwest coast of India. *Reg. Stud. Mar. Sci.* 18, 113–121.
- Arunpandi, N., Jyothibabu, R., Jagadeesan, L., Gireeshkumar, T. R., Karnan, C., Naqvi, S.W.A., 2017. Noctiluca and copepods grazing on the phytoplankton community in a nutrient-enriched coastal environment along the southwest coast of India. *Environ. Monit. Assess.* 189. <https://doi.org/10.1007/s10661-017-6061-9>
- Azzoni, R., Giordani, G., Viaroli, P., 2005. Iron-sulphur-phosphorus interactions: Implications for sediment buffering capacity in a mediterranean eutrophic lagoon (Sacca di Goro, Italy). *Hydrobiologia* 550, 131–148. <https://doi.org/10.1007/s10750-005-4369-x>
- Badesab, F., Gaikwad, V., Gireesh Kumar, T., Naikgaonkar, O., Deenadayalan, K., Samiksha, S. V., Dinesh Kumar, P., Loveson, V. J., Iyer, S., Khan, A., Udayakrishnan, P., Sardar, A., 2018. Magnetic tracing of sediment dynamics of mudbanks off southwest coast of India. *Environ. Earth Sci.* 77, 0. <https://doi.org/10.1007/s12665-018-7807-6>
- Balachandran, K. K., 2004. Does subterranean flow initiate mud banks off the southwest coast of India? *Estuar. Coast. Shelf Sci.* 59, 589–598.
- Balachandran, K. K., Joseph, T., Nair, M., Sankaranarayanan, V. N., Kesavadas, V., Sheeba, P., 2003. Geochemistry of surficial sediments along the central southwest coast of India - Seasonal changes in regional distribution. *J. Coast. Res.* 19, 664–683.
- Balzer, W., 1982. On the distribution of iron and manganese at the sediment/water interface: thermodynamic versus kinetic control. *Geochim. Cosmochim. Acta* 46, 1153–1161. [https://doi.org/10.1016/0016-7037\(82\)90001-1](https://doi.org/10.1016/0016-7037(82)90001-1)

- Berner, R. A., 1984. Sedimentary pyrite formation. *Am. J. Sci.* 48, 605–615. <https://doi.org/10.2475/ajs.268.1.1>
- Berner, R. A., 1981. A new geochemical classification of sedimentary environments. *J. Sediment. Perology* 51, 359–365.
- Bristow, R. C., 1938. Cochin Harbour Development: History of Mud bank, Vol.1. Cochin Govt. Press, Ernakulam, India, 174.
- Burdige, D. J., 1993. The biogeochemistry of manganese and iron reduction in marine sediments. *Earth Sci. Rev.* 35, 249–284. [https://doi.org/10.1016/0012-8252\(93\)90040-E](https://doi.org/10.1016/0012-8252(93)90040-E)
- Canfield, D. E., 1989. Reactive iron in marine sediment. *Geochim. Cosmochim. Acta.* 53, 619-632.
- Canfield, D. E., Berner, R. A., 1987. Dissolution and pyritization of magnetite in anoxic marine sediments. *Geochim. Cosmochim. Acta.* 51, 645-660.
- Canfield, D. E., Raiswell, R., Bottrell, S., 1992. The reactivity of sedimentary iron minerals toward sulfide. *Am. J. Sci.* 292, 659–683. <https://doi.org/10.2475/ajs.292.9.659>
- Canfield, D. E., Raiswell, R., Westrich, J. T., Reaves, C. M., Berner, R. A., 1986. The use of chromium reduction in the analysis of reduced inorganic sulfur in sediments and shales. *Chem. Geol.* 54, 149–155. [https://doi.org/10.1016/0009-2541\(86\)90078-1](https://doi.org/10.1016/0009-2541(86)90078-1)
- Chanton, J. P., Martens, C. S., Goldhaber, M. B., 1987. Biogeochemical cycling in an organic-rich coastal marine basin. 8. A sulfur isotopic budget balanced by differential diffusion across the sediment-water interface. *Geochim. Cosmochim. Acta* 51, 1201–1208. [https://doi.org/10.1016/0016-7037\(87\)90212-2](https://doi.org/10.1016/0016-7037(87)90212-2)
- Clarkson, M. O., Poulton, S. W., Guilbaud, R., Wood, R. A., 2014. Assessing the utility of Fe/Al and Fe-speciation to record water column redox conditions in carbonate-rich sediments. *Chem. Geol.* 382, 111–122. <https://doi.org/10.1016/j.chemgeo.2014.05.031>
- CMFRI Bulletin., 1984. Mudbanks of Kerala Coast. Central Marine Fisheries Research Institute Bulletin No. 31, Kochi-18.
- Croot, P. L., Heller, M. I., Wuttig, K., 2019. Redox Processes Impacting the Flux of Iron(II) from Shelf Sediments to the OMZ along the Peruvian Shelf. *ACS Earth and Space Chemistry* 3, 537-549.
- Cui, M., Ma, A., Qi, H., Zhuang, X., Zhuang, G., 2014. Anaerobic oxidation of methane: An "active" microbial process. *Microbiology open* 4, 1–11. <https://doi.org/10.1002/mbo3.232>
- Damodaran, R., Hridayanathan, C., 1966. Studies on the mud banks of the Kerala Coast. *Bull. Dep. Mar. Sci. Univ. Cochin*, 6, 61-68.
- Dill, H. G., Siegfanz, G., Marchig, V., 1994. Mineralogy and chemistry of metalliferous muds forming the topstratum of a massive sulfide-metalliferous sediment sequence from east pacific rise 18°s: Its origin and implications concerning the formation of ochrous sediments in cyprus-type deposits. *Mar. Georesources Geotechnol.* 12, 159–180.
- Dinesh, A. C., Jayaprakash, C., 2008. Zaherite the key mineral. *Curr. Sci.* 95, 962–967.

- Dora, Y. L., Damodaran, R., Jos Anto, V., 1968. Texture of the Narakal Mud Bank Sediments. Bull. Dept. Mar. Biol. Oceanogr. 4, 1-10.
- Folk, R. L., 1980. Petrology of sedimentary rocks. Hemphil publishing company, Austin, texas, 78703.
- Follett, E, A, C., 1965. The retention of amorphous, colloidal "Ferric hydroxide" by kaolinites. J. Soil Sci. 16, 334–341.
- Froelich, P. N., Klinkhammer, G. P., Bender, M. L., Luedtke, N. A., Heath, G. R., Cullen, D., Dauphin, P., Hammond, D., Hartman, B., Maynard, V., 1979. Early oxidation of organic matter in pelagic sediments of the eastern equatorial Atlantic: suboxic diagenesis. Geochim. Cosmochim. Acta 43, 1075–1090.
- Garrels, R. M., Christ, C., 1965. Solutions, minerals, and equilibria. New York; Harper Row 450.
- Gibbs, R.J., 1977. Geological Society of America Bulletin Transport phases of transition metals in the Amazon and Yukon Rivers. Geol. Soc. Am. Bull. [https://doi.org/10.1130/0016-7606\(1977\)88<829](https://doi.org/10.1130/0016-7606(1977)88<829)
- Gireeshkumar, T. R., Mathew, D., Pratihary, A.K., Naik, H., Narvekar, K. U., Araujo, J., Balachandran, K. K., Muraleedharan, K. R., Thorat, B., Nair, M., Naqvi, S.W.A., 2017. Influence of upwelling induced near shore hypoxia on the Alappuzha mud banks, South West Coast of India. Cont. Shelf Res. 139, 1–8. <https://doi.org/10.1016/j.csr.2017.03.009>
- Gireeshkumar, T. R., Mathew, D., Udayakrishnan, P. B., Shameem, K., Fahad Fathin, K. P., Furtado, C. M., Deepulal P. M., Nair, M., Balachandran, K. K., 2020. Montmorillonite and phosphorus enrichment in sediments as the causative factor for the formation of mud banks along the southwest coast of India. Regional Studies in Marine Science. 40, 101517. <https://doi.org/10.1016/j.rsma.2020.101517>
- Goldhaber, M. B., Kaplan, I. R., 1974. The sulfur cycle, in Goldberg, E.D., editor, The Sea, v. 5: New York, WileyInterscience, P. 569-655.
- Grasshoff, K., Ehrhardt, M., Kremling, K., 1983. Methods of sea water analysis, 2nd edition. Verlag Chemie, Weinheim.
- Greenland, D. J., 1975. Charge characteristics of some kaolinite-iron hydroxide complexes. Clay Miner. 10:407-416.
- Greenland, D. J., Mott, C.J.B., 1978. Iron hydroxides and clay surfaces. In: Greenland, D.J., Hayes, M.H.B. (Eds.), The Chemistry of Soil Constituents. Wiley, Chichester, 321-353.
- Groeningen, N. V., Thomasarrigo, L. K., Byrne, J. M., Kappler, A., Christl, I., Kretzschmar, R., 2020. Interactions of ferrous iron with clay mineral surfaces during sorption and subsequent oxidation. Environmental Sci. Process. iMPACTS 22, 1355–1367. <https://doi.org/10.1039/d0em00063a>
- Gu, X. Z., Chen, K. N., Zhang, L., Fan, C. X., 2016. Preliminary evidence of nutrients release from sediment in response to oxygen across benthic oxidation layer by a long-term field trial. Environ. Pollut. 219, 656–662. doi: 10.1016/j. envpol.2016.06.044

- Gupta, G.V. M., Sudheesh, V., Sudharma, K. V, Saravanane, N., Dhanya, V., Dhanya, K. R., Lakshmi, G., Sudhakar, M., Naqvi, S.W. A., 2016. Evolution to decay of upwelling and associated biogeochemistry over the southeastern Arabian Sea shelf. 121, 159-175.
- Hedges, J. I., Keil, R. G., Giddings, J. C., Tsamakis, E., Fuh, CB, 2003. Mineralogical and textural controls on the organic composition of coastal marine sediments: Hydrodynamic separation using SPLITT-fractionation. *Geochim. Cosmochim. Acta* 58, 879–893. [https://doi.org/10.1016/0016-7037\(94\)90512-6](https://doi.org/10.1016/0016-7037(94)90512-6).
- Hsu, F. H., Su, C. C., Wang, C. H., Lin, S., Liu, J., Huh, C. A., 2014. Accumulation of terrestrial organic carbon on an active continental margin offshore southwestern Taiwan: source-to-sink pathways of river-borne organic particles. *J. Asian Earth Sci.* 91, 163–173
- Hyacinthe, C., Bonneville, S., Van Cappellen, P., 2006. Reactive iron(III) in sediments: Chemical versus microbial extractions. *Geochim. Cosmochim. Acta* 70, 4166–4180. <https://doi.org/10.1016/j.gca.2006.05.018>
- Hyacinthe, C., Van Cappellen, P., 2004. An authigenic iron phosphate phase in estuarine sediments: Composition, formation and chemical reactivity. *Mar. Chem.* 91, 227–251. <https://doi.org/10.1016/j.marchem.2004.04.006>
- Jensen, H. S., Mortensen, P. B., Anderson, F. O., Rasmussen, E., Jensen, A., 1995. Phosphorus cycling in a coastal marine sediment, Aarhus Bay, Denmark. *Limnol. Oceanogr.* 40, 908-917.
- Johnson, K.S., Chavez, F.P., Friederich, G.E., 1999. Continental-shelf sediment as a primary source of iron for coastal phytoplankton. *Nature* 398, 697–700. <https://doi.org/10.1038/19511>
- Jørgensen, B., Bang, M., Blackburn, T., 1990. Anaerobic mineralization in marine sediments from the Baltic Sea-North Sea transition. *Mar. Ecol. Prog. Ser.* 59, 39–54. <https://doi.org/10.3354/meps059039>
- Jørgensen, B. B., 1977. The sulfur cycle of a coastal marine sediment (Limfjorden, Denmark). *Limnol. Oceanogr.* 22, 814–832. <https://doi.org/10.4319/lo.1977.22.5.0814>
- Jørgensen, B. B., 1982. Mineralization of organic matter in the sea bed-the role of sulfate reduction. *Nature* 296, 643-645.
- Jyothibabu, R., Balachandran, K. K., Jagadeesan, L., Karnan, C., Arunpandi, N., 2018. Mud Banks along the southwest coast of India are not too muddy for plankton. *Sci. Rep.* 1–13. <https://doi.org/10.1038/s41598-018-20667-9>
- Jyothibabu, R., Karnan, C., Jagadeesan, L., Arunpandi, N., 2020. Ecological responses of autotrophic microplankton to the eutrophication of the coastal upwelling along the Southwest coast of India. *Environ. Sci. Pollut. Res.*
- Karnan, C., Jyothibabu, R., Arunpandi, N., Jagadeesan, L., Muraleedharan, K. R., Pratihari, A. K., Naqvi, S. W. A. 2017. Discriminating the biophysical impacts of coastal upwelling and mud banks along the southwest coast of India. *Journal of Marine Systems*, 172, 24–42.
- Knebel, H. J., Kelly, J. C., Whetten, J. T., 1968. Clay minerals of the Columbia river: a qualitative, quantitative and statistical evaluation. *J. Sediment Pet.* 38, 600-611.

- Konhauser, K., 2006. Introduction to Geomicrobiology. Malden: Black- well Publishing
- Krom, M. D., Berner, R. A., 1980. Adsorption of phosphate in anoxic marine sediments. *Limnol. Oceanogr.* 25, 797-806.
- Kurup, P. G., 1972. Littoral currents in relations to the mud bank formation along the coast of Kerala. *Mahasagar* 5 (3), 158-162.
- Kurup, P. G., 1977. Studies on the physical aspects of the mud banks along the Kerala coasts with special reference to the Purakad mud bank. *Bulletin of Department of Marine Science, University of Cochin*, 7, 1-72.
- Laufer, K., Byrne, J.M., Glombitza, C., Schmidt, C., Jørgensen, B.B., Kappler, A., 2016. Anaerobic microbial Fe(II) oxidation and Fe(III) reduction in coastal marine sediments controlled by organic carbon content. *Environ. Microbiol.* 18, 3159–3174. <https://doi.org/10.1111/1462-2920.13387>
- Leslie, B.W., Hammond, D.E., Berelson, W.M., Lund, S.P., 1990a. Diagenesis in Anoxic Sediments From the California Continental Borderland and Its Influence on Iron , Sulfur , and Magnetite Behavior. *J. Geophys. Res.* 95, 4453–4470.
- Leslie, B.W., Lund, S.P., Hammond, D.E., 1990b. Rock Magnetic Evidence for the Dissolution and Authigenic Growth of Magnetic Minerals Within Anoxic Marine Sediments. *J. Geophys. Res.* 95, 4437–4452.
- Li, C., Yang, S., Lian, E., Wang, Q., Fan, D., Huang, X., 2016. Chemical speciation of iron in sediments from the Changjiang Estuary and East China Sea: Iron cycle and paleoenvironmental implications. *Quat. Int.* 452, 116–128. <https://doi.org/10.1016/j.quaint.2016.07.014>
- Lyons, T. W., 1997. Sulfur isotopic trends and pathways of iron sulfide formation in upper holocene sediments of the anoxic black sea. *Geochim. Cosmochim. Acta* 61, 3367–3382. [https://doi.org/10.1016/S0016-7037\(97\)00174-9](https://doi.org/10.1016/S0016-7037(97)00174-9)
- Lyons, T.W., Severmann, S., 2006. A critical look at iron paleoredox proxies: New insights from modern euxinic marine basins. *Geochim. Cosmochim. Acta* 70, 5698–5722. <https://doi.org/10.1016/j.gca.2006.08.021>
- Madhu, N. V., Anil, P., Gireeshkumar, T.R., Muraleedharan, K.R., Kiran, K., Vishal, CR, 2020. Phytoplankton characterization in the Alappuzha mud banks during the pre- / post phases of a red-tide , *Prorocentrum shikokuense* Hada. *Reg. Stud. Mar. Sci.* 40, 101486. <https://doi.org/10.1016/j.rsma.2020.101486>
- Mallik, T. K., Mukherji, K. K., Ramachandran, K. K., 1988. Sedimentology of the Kerala mud banks (fluid muds?). *Mar. Geol.* 80, 99–118.
- Mallik, T.K., Ramachandran, K.K., 1984. Mudbanks of Kerala Coast - a state of the art report. Report of State Committee on Science and Technology. Government of Kerala, 21.
- Mallik, T. K., Vasudevan, V., Verghese, P. A, Machado, T., 1987. The black sand placer deposits of kerala beach , southwest india. *Mar. Geol.* 77, 129–150.

- März, C., Hoffmann, J., Bleil, U., de Lange, G.J., Kasten, S., 2008. Diagenetic changes of magnetic and geochemical signals by anaerobic methane oxidation in sediments of the Zambezi deep-sea fan (SW Indian Ocean). *Mar. Geol.* 255, 118–130. <https://doi.org/10.1016/j.margeo.2008.05.013>
- Mathew, D., Gireeshkumar, T. R., Balachandran, K. K., Udayakrishnan, P. B., Shameem, K., Deepulal, P. M., Nair, M., Madhu, N. V, Muraleedharan, K. R., 2020. Influence of hypoxia on phosphorus cycling in Alappuzha mud banks , southwest coast of India. *Reg. Stud. Mar. Sci.* 34, 101083. <https://doi.org/10.1016/j.rsma.2020.101083>
- Mathew, D., Gireeshkumar, T.R., Udayakrishnan, P.B., Muraleedharan, K.R., Madhu, N.V., Nair, M., C.Revichandran, Balachandran, KK, 2019. Inter-annual variations in the hydrochemistry of Alappuzha mud banks, southwest coast of India. *Cont. Shelf Res.* 177, 42–49. <https://doi.org/10.1016/j.csr.2019.03.008>
- Mathew, J., 1992. Wave-Mud interaction in mud banks. Ph.D. Thesis, Cochin University of Science and Technology.
- Mathew, J., Baba, M., 1995. Mudbanks of SW coast of India II: wave-mud interaction. *Journal of Coastal Research* 11, 179–187.
- Mathew, K. J., Gopinathan, C. P., 2000. Study of mud banks of the Kerala coast a retrospect. *Mar. Fish. Res. Manag.*, 117-189.
- Miot, J., Benzerara, K., Morin, G., Bernard, S., Beyssac, O., Larquet, E., Kappler, A., Guyot, F., 2009. Transformation of vivianite by anaerobic nitrate-reducing iron-oxidizing bacteria. *Geobiology* 7, 373-384.
- Morse, E., 1992. Carbon / sulphur / iron relationships in upwelling sediments. *Geol. Soc. Spec. Publ.* 247–255.
- Muraleedharan, K. R, Dinesh Kumar, P. K., Prasanna Kumar, S., John, S., Srijith, B., Anil Kumar, K., Naveen Kumar, K., Gautham, S., Samiksha, V., 2017b. Correction to: Formation Mechanism of Mud Bank Along the Southwest Coast of India. *Estuaries and Coasts* 1. <https://doi.org/10.1007/s12237-017-0343-x>
- Muraleedharan, K. R., Dinesh Kumar, P.K., Prasanna Kumar, S., Srijith, B., John, S., Naveen Kumar, K.R., 2017a. Observed salinity changes in the Alappuzha mud bank, southwest coast of India and its implication to hypothesis of mudbank formation. *Cont. Shelf Res.* 137, 39–45. <https://doi.org/10.1016/j.csr.2017.01.015>
- Murty, A. V. S., Rao, D. S., Regunathan, A., Gopinathan, C. P., Mathew, K. J., 1984. Hypotheses on mudbanks. *Bulletin No. 31.* Cochin: Central Marine Fisheries Research Institute, 8-17.
- Murthy, M.V.N., 1975. A review of mineral resources of Kerala and their utilization. *Proc. Symp. on Mineral Resources of Kerala and their Utilization*, State Planning Board, Govt. of Kerala, 166 pp .
- Nair, R.R., 1976. Unique Mud Banks, Kerala, Southwest India. *The American Association of Petroleum Geologists Bulletin.*60 (4), 616-621.
- Nair, R. R., Murty, P. S. N., Varadachari, V.V. R., 1966. Physical and chemical aspects of mud deposit of Vypeen beach. *IIOE Newsletter*, 4(2):1-10.

- Naqvi, S.W. A., Jayakumar, D. A., Narveka, P. V., Naik, H., Sarma, V. V. S. S., D'Souza, W., Joseph, S., and George, M. D., 2000. Increased marine production of N₂O due to intensifying anoxia on the Indian continental shelf, *nature*, 408, 346–349.
- Narayana, A. C., Jago, C. F., Manojkumar, P., Tatavarti, R., 2008. Nearshore sediment characteristics and formation of mudbanks along the Kerala coast, southwest India. *Estuar. Coast. Shelf Sci.* 78, 341–352.
- Nickel, M., Vandieken, V., Brüchert, V., Jørgensen, B.B., 2008. Microbial Mn(IV) and Fe(III) reduction in northern Barents Sea sediments under different conditions of ice cover and organic carbon deposition. *Deep. Res. Part II Top. Stud. Oceanogr.* 55, 2390–2398. <https://doi.org/10.1016/j.dsr2.2008.05.003>
- Otero, M.I., Franco-Uría, A., Alonso, A.A., Balsa-Canto, E., 2010. Dynamic multi-compartmental modelling of metal bioaccumulation in fish: Identifiability implications. *Environ. Model. Softw.* 25, 344–353. <https://doi.org/10.1016/j.envsoft.2009.08.009>.
- Parvathi, A., Jasna, V., Aswathy, V.K., Nathan, V.K., Aparna, S., Balachandran, KK, 2019. Microbial diversity in a coastal environment with co-existing upwelling and mud-banks along the south west coast of India. *Mol. Biol. Rep.* <https://doi.org/10.1007/s11033-019-04766-y>
- Poulton, S.W., Canfield, D. E., 2005. Development of a sequential extraction procedure for iron: Implications for iron partitioning in continentally derived particulates. *Chem. Geol.* 214, 209–221. <https://doi.org/10.1016/j.chemgeo.2004.09.003>
- Poulton, S. W., Canfeld, D. E., 2011. Ferruginous conditions: A dominant feature of the ocean through Earth's history. *Elements* 7, 107–112. <https://doi.org/10.2113/gselements.7.2.107>
- Poulton, S. W., Fralick, P. W., Canfield, D.E., 2004b. The transition to a sulphidic ocean , 1 . 84 billion years ago. *Nature* 431, 173–177. <https://doi.org/10.1038/nature02863.1>.
- Poulton, S. W., Krom, M. D., Raiswell, R., 2004a. A revised scheme for the reactivity of iron (oxyhydr)oxide minerals towards dissolved sulfide. *Geochim. Cosmochim. Acta* 68, 3703–3715. <https://doi.org/10.1016/j.gca.2004.03.012>
- Poulton, S.W., Raiswell, R., 2005. Chemical and physical characteristics of iron oxides in riverine and glacial meltwater sediments. *Chem. Geol.* 218, 203–221. <https://doi.org/10.1016/j.chemgeo.2005.01.007>
- Poulton, S.W., Raiswell, R., 2002. The low-temperature geochemical cycle of iron: From continental fluxes to marine sediment deposition. *Am. J. Sci.* 302, 774–805. <https://doi.org/10.2475/ajs.302.9.774>
- Pourbaix, M., 1974. Atlas of electrochemical equilibria in aqueous solutions. 2nd English Ed. Nationalassociation of corrosionengineers,Houston, Texas.
- Prasanna Kumar, S., Dineshkumar, P., Muraleedharan, K.R., George, G., Mathew, D., Kripa, V., Jeyabaskaran, R., Ramaiah, N., Gopalakrishnan, A., 2018. Mudbanks and fisheries along the Kerala coast – myth and reality. *Curr. Sci.* 115, 1–7.

- Purandara, B. K., 1990. Provenance, Sedimentation and geochemistry of the modern sediments of the mud banks off the central Kerala Coast, India. Ph. D Thesis. Cochin University of Science and Technology. Indian Journal of Marine Science, 8, 78-84.
- Purandara, B. K., Dora, Y.L., 1987. Proc. Nat. Sem. Estuarine Management. Trivandrum, pp.449-452.
- Raiswell, R., Canfield, D. E., 1998. Sources of iron for pyrite formation in marine sediments. Am. J. Sci. 298, 219–245. <https://doi.org/10.2475/ajs.298.3.219>
- Raiswell, R., Canfield, D. E., Berner, R. A., 1994. A comparison of iron extraction methods for the determination of degree of pyritization and the recognition of iron-limited pyrite formation. Chem. Geol. 111, 101–110. [https://doi.org/10.1016/0009-2541\(94\)90084-1](https://doi.org/10.1016/0009-2541(94)90084-1)
- Raiswell, R., Newton, R., Wignall, P.B., 2001. An indicator of water-column anoxia: Resolution of biofacies variations in the Kimmeridge clay (Upper Jurassic, UK). J. Sediment. Res. 71, 286–294.
- Ramachandran, K. K., Samsuddin, M., 1991. Removal of sediments from the Alleppey nearshore region during post-mudbank formation. Proceedings of the Indian Academy of Sciences (Earth and Planetary) 100, 195-203.
- Roberts, A. P., 2015. Magnetic mineral diagenesis. Earth-Science Rev. 151, 1-47. <https://doi.org/10.1016/j.earscirev.2015.09.010>
- Rothe, M., Kleeberg, A., Grüneberg, B., Friese, K., Pérez-Mayo, M., Hupfer, M., 2015. Sedimentary sulphur:iron ratio indicates vivianite occurrence: A study from two contrasting freshwater systems. PLoS One 10, 1–18.
- Rothe, M., Kleeberg, A., Hupfer, M., 2016. The occurrence, identification and environmental relevance of vivianite in waterlogged soils and aquatic sediments. Earth-Science Reviews 158, 51-64.
- Samiksha, S. V., Vethamony, P., Rogers, W.E., Pednekar, P.S., Babu, M.T., Dineshkumar, P.K., 2017. Wave energy dissipation due to mudbanks formed off southwest coast of India. Estuar. Coast. Shelf Sci. 196, 387–398. <https://doi.org/10.1016/j.ecss.2017.07.018>
- Schenau, S.J., Passier, H.F., Reichart, G.J., De Lange, G.J., 2002. Sedimentary pyrite formation in the Arabian Sea. Mar. Geol. 185, 393–402. [https://doi.org/10.1016/S0025-3227\(02\)00183-4](https://doi.org/10.1016/S0025-3227(02)00183-4)
- Schulz, H. D., Zabel, M., 2006. Marine Geochemistry 2nd revised , updated and extended edition. Springer, Berlin, Heidelberg.
- Shynu, R., Rao, V. P., Samiksha, S. V, Vethamony, P., Naqvi, S.W.A., Kessarkar, P. M., Babu, M.T., Dineshkumar, P.K., 2017. Estuarine, Coastal and Shelf Science Suspended matter and fluid mud off Alleppey, southwest coast of India. Estuar. Coast. Shelf Sci. 185, 31-43.
- Slomp, C. P., Mort, H. P., Jilbert, T., Reed, D. C., Gustafsson, B. G., Wolthers, M., 2013. Coupled dynamics of iron and phosphorus in sediments of an oligotrophic coastal basin and the impact of anaerobic oxidation of methane. PLoS One 8, e62386.

- Slomp, C.P., Van der Gaast, S.J., Van Raaphorst, W., 1996. Phosphorus binding by poorly crystalline iron oxides in North Sea sediments. *Mar. Chem.* 52, 55–73. [https://doi.org/10.1016/0304-4203\(95\)00078-X](https://doi.org/10.1016/0304-4203(95)00078-X)
- Slotznick, S.P., Sperling, E.A., Tosca, N.J., Miller, A.J., Clayton, K.E., van Helmond, NAGM, Slomp, C.P., Swanson-Hysell, N.L., 2020. Unraveling the Mineralogical Complexity of Sediment Iron Speciation Using Sequential Extractions. *Geochemistry, Geophysics, Geosystems* 21, e2019GC008666.
- Straub, K.L., Benz, M., Schink, B., Widdel, F., 1996. Anaerobic, nitrate-dependent microbial oxidation of ferrous iron. *Appl. Environ. Microbiol.* 62, 1458–1460.
- Stumm, W., Morgan, J.J., 1981. *Aquatic Chemistry*, John Wiley and Sons, New York.
- Tatavarti, R., Narayana, A. C., Manoj Kumar, P., Chand, S., 1999. Mudbank regime off the Kerala coast during monsoon and non-monsoon seasons. *Proc. Indian Acad. Sci. Earth Planet. Sci.* 108, 57–68.
- Tatavarti, R., Narayana, A. C., Ravisankar, M., Manojkumar, P., 1996. Mudbank dynamics field evidence of edge waves and far infra-gravity waves. *Current Science*.
- Taylor, K.G., Konhauser, K.O., 2011. In earth surface systems: A major player in chemical and biological processes. *Elements* 7, 83–88. <https://doi.org/10.2113/gselements.7.2.83>
- Tessier, A., Campbell, P.G.C., Bisson, M., 1979. Sequential Extraction Procedure for the Speciation of Particulate Trace Metals. *Anal. Chem.* 51, 844–851. <https://doi.org/10.1021/ac50043a017>
- Thamdrup, B., 2000. Bacterial Manganese and Iron Reduction. *Advances Microb. Ecol.* 41-84.
- Vandieken, V., Nickel, M., Jørgensen, B.B., 2006. Carbon mineralization in Arctic sediments northeast of Svalbard: Mn(IV) and Fe(III) reduction as principal anaerobic respiratory pathways. *Mar. Ecol. Prog. Ser.* 322, 15–27. <https://doi.org/10.3354/meps322015>
- Whitney, P.R., 1975. Relationship of manganese-iron oxides and associated heavy metals to grain size in stream sediments. *J. Geochemical Explor.* 4, 251–263. [https://doi.org/10.1016/0375-6742\(75\)90005-9](https://doi.org/10.1016/0375-6742(75)90005-9)
- Widdel, F., Schnell, S., Heising, S., Ehrenreich, A., Assmus, B., Schink, B., 1993. Ferrous iron oxidation by anoxygenic phototrophic bacteria. *Nature* 362, 834–836. <https://doi.org/10.1038/362834a0>
- Zhu, M.X., Hao, X.C., Shi, X.N., Yang, G.P., Li, T., 2012. Speciation and spatial distribution of solid-phase iron in surface sediments of the East China Sea continental shelf. *Appl. Geochemistry* 27, 892–905. <https://doi.org/10.1016/j.apgeochem.2012.01.004>
- Zhu, M.X., Huang, X.L., Yang, G.P., Chen, L.J., 2015. Iron geochemistry in surface sediments of a temperate semi-enclosed bay, North China. *Estuar. Coast. Shelf Sci.* 165, 25–35. <https://doi.org/10.1016/j.ecss.2015.08.018>

Figure captions:

Figure 1 Map of the study region showing locations of sampling stations (M1, M2, and M3) in Alappuzha mud banks. The discontinuous white line indicates the approximate boundary of the persistent mud bank site. The red dots (upper left panel) reported mud bank locations along the southwest coast of India

Figure 2 Fe speciation scheme (Poulton and Canfield, 2005) adopted for the present study.

Figure 3 Seasonal variability of temperature, salinity and dissolved oxygen in the study region.

Figure 4 Distribution of sand, silt and clay in surface sediments of the Alappuzha mud bank.

Figure 5 Distribution of total organic carbon (TOC), total nitrogen (TN), total sulfur (TS) and total phosphorus (TP) in surface sediment in the study region.

Figure 6 a Seasonal distribution of various Fe forms (Fe_{carb} , Fe_{ox1} , Fe_{ox2} , Fe_{mag} , Fe_{PRS} , Fe_{pyr} & Fe_U) in mud bank sediments; **b.** percentage distribution of highly reactive Fe (Fe_{HR}), poorly reactive Fe (Fe_{PR}) and unreactive Fe (Fe_U) in mud bank sediments.

Figure 7 a & b Various sedimentary Fe forms in response to oxygen profile in mud bank.

Table 1 Distribution of total iron (Fe_T), Fe(III)_{HR}/Fe_{HR}, Fe_{HR}/Fe_T, Fe_{pyr}/Fe_{HR}, and Mn in surface sediments

Sampling Date	Fe _T (mgg ⁻¹)			Fe(III) _{HR} /Fe _{HR}			Fe _{HR} /Fe _T			Fe _{pyr} /Fe _{HR}			Mn (μgg ⁻¹)		
	M1	M2	M3	M1	M2	M3	M1	M2	M3	M1	M2	M3	M1	M2	M3
20-Apr-16	62.85±0.27	67.41±0.55	62.85±0.28	0.76	0.79	0.79	0.49	0.49	0.49	0.11	0.07	0.08	-	128±0.35	148±0.61
11-May-16	61.14±0.18	74.34±0.37	59.13±0.66	0.79	0.77	0.79	0.49	0.43	0.57	0.12	0.07	0.07	142±0.51	136±0.35	135±0.45
08-Jun-16	59.85±0.17	65.28±0.13	66.6±0.18	0.77	0.78	0.79	0.47	0.49	0.49	0.11	0.08	0.08	150±0.18	119±0.25	113±0.27
14-Jun-16	66.99±0.56	69.93±0.41	53.34±0.37	0.76	0.77	0.78	0.43	0.46	0.61	0.1	0.07	0.07	122±0.55	93±0.45	92±0.41
24-Jun-16	58.9±0.41	58.94±0.36	59.3±0.44	0.75	0.78	0.78	0.49	0.56	0.57	0.11	0.07	0.09	89±0.32	94±0.21	91±0.44
10-Jul-16	59.45±0.38	56.06±0.18	62.2±0.35	0.77	0.8	0.8	0.51	0.52	0.55	0.12	0.09	0.08	95±25	91±0.32	77±0.43
27-Jul-16	58.34±0.41	58.3±0.21	59.11±0.22	0.8	0.8	0.83	0.53	0.61	0.59	0.08	0.12	0.06	85±0.55	83±0.28	91±0.18
10-Aug-16	62.27±0.31	59.85±43	57.45±0.36	0.82	0.8	0.83	0.51	0.54	0.59	0.08	0.11	0.06	-	-	-
26-Aug-16	62.56±0.43	61.36±0.23	55.56±0.28	0.83	0.81	0.84	0.56	0.58	0.62	0.07	0.09	0.06	70±0.53	72±0.35	74±0.25
Mean	61.37	63.5	59.5	0.78	0.79	0.8	0.5	0.52	0.56	0.1	0.09	0.07	107.57	102	102.63
± SD	2.52	5.76	3.76	0.03	0.01	0.02	0.03	0.05	0.04	0.02	0.02	0.01	28.33	21.35	25.18
Fluid mud	-	55.52±0.8	-	-	-	-	-	-	-	-	-	-	-	92±0.4	-

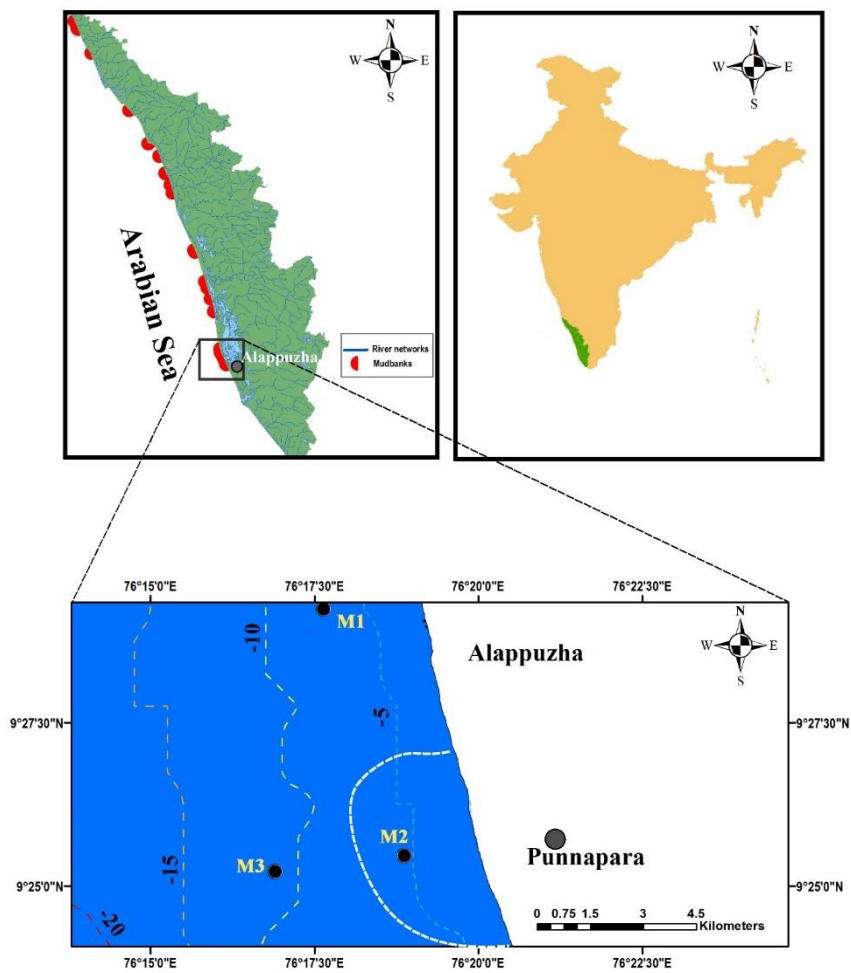


Figure 1

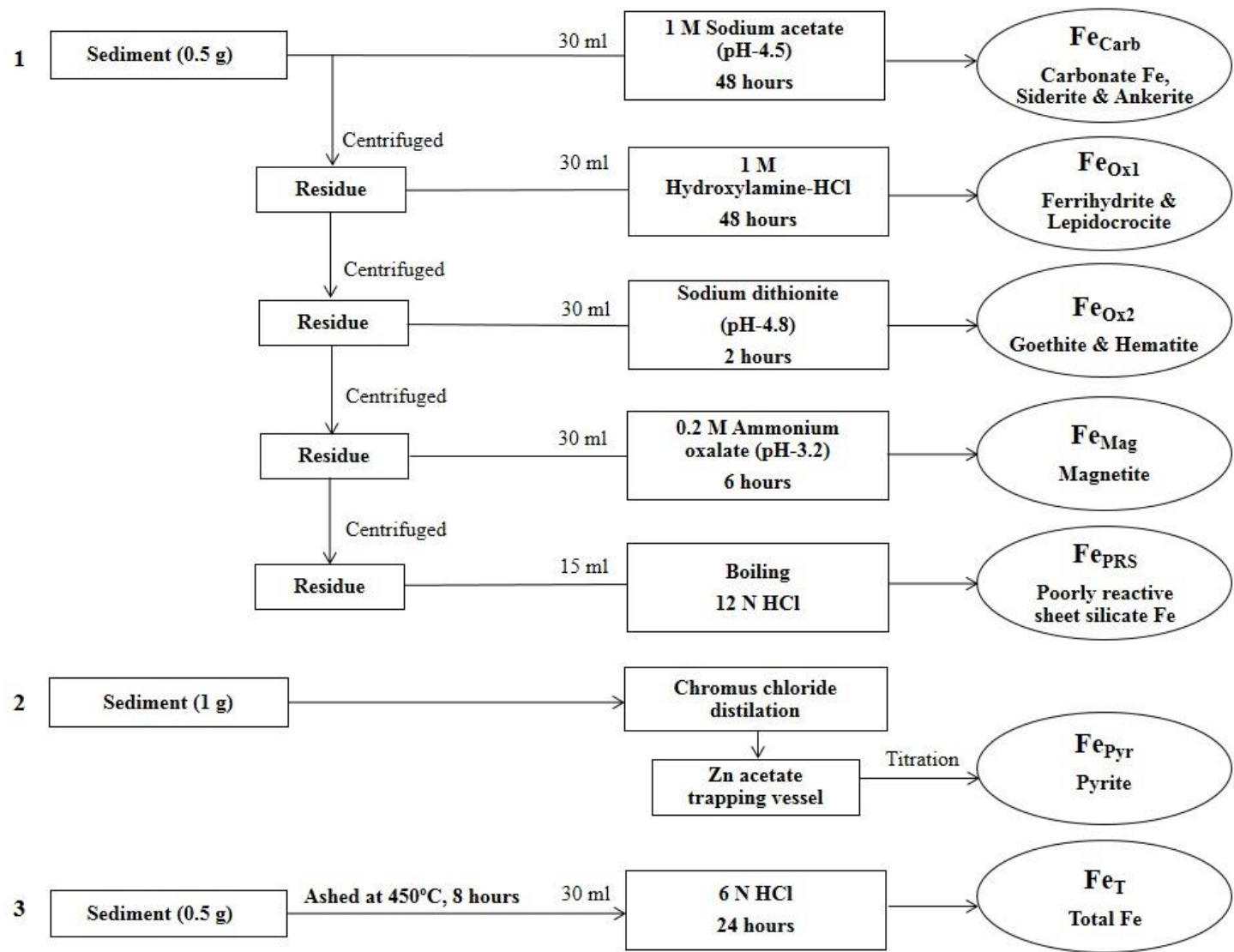


Figure 2

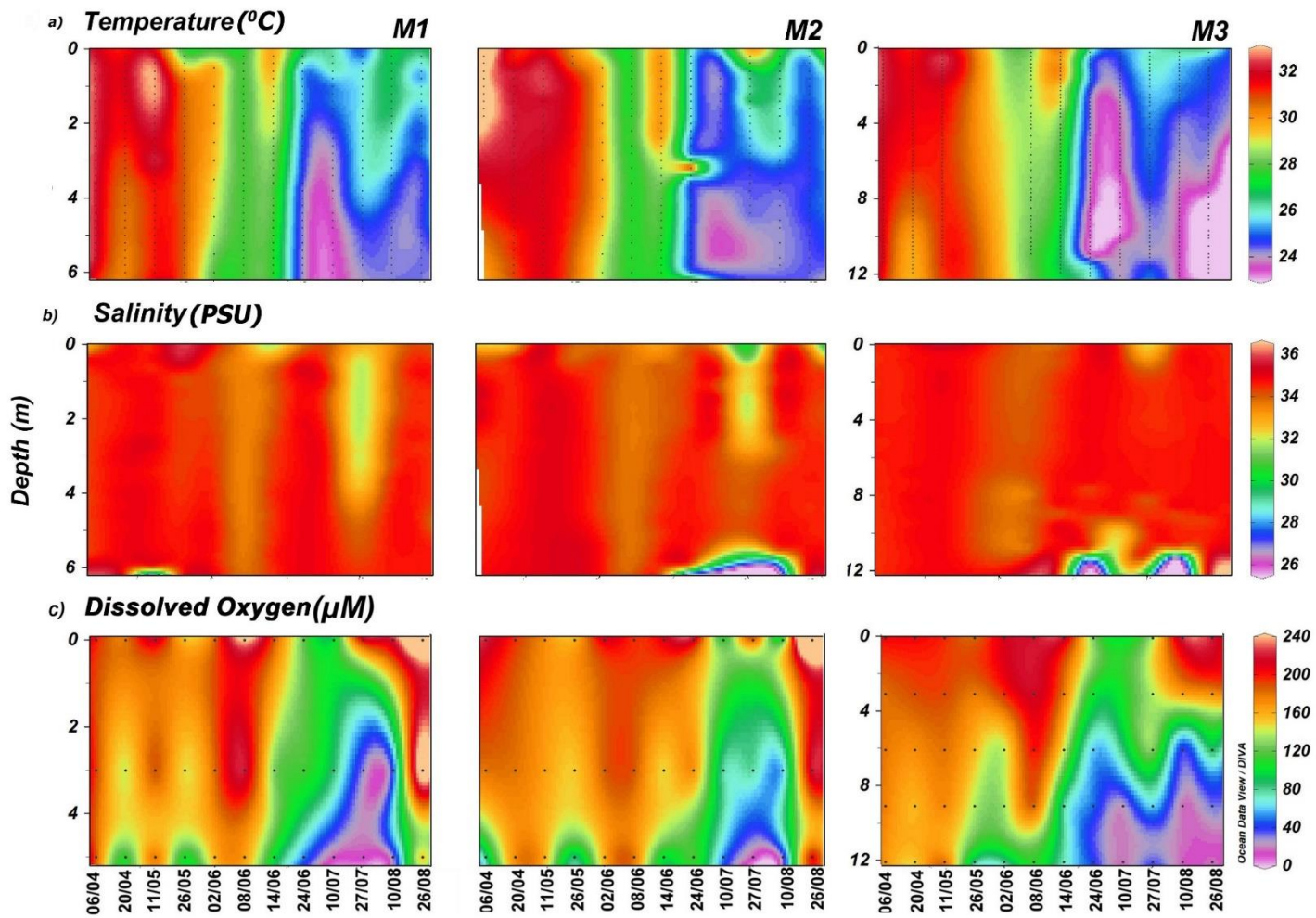


Figure 3

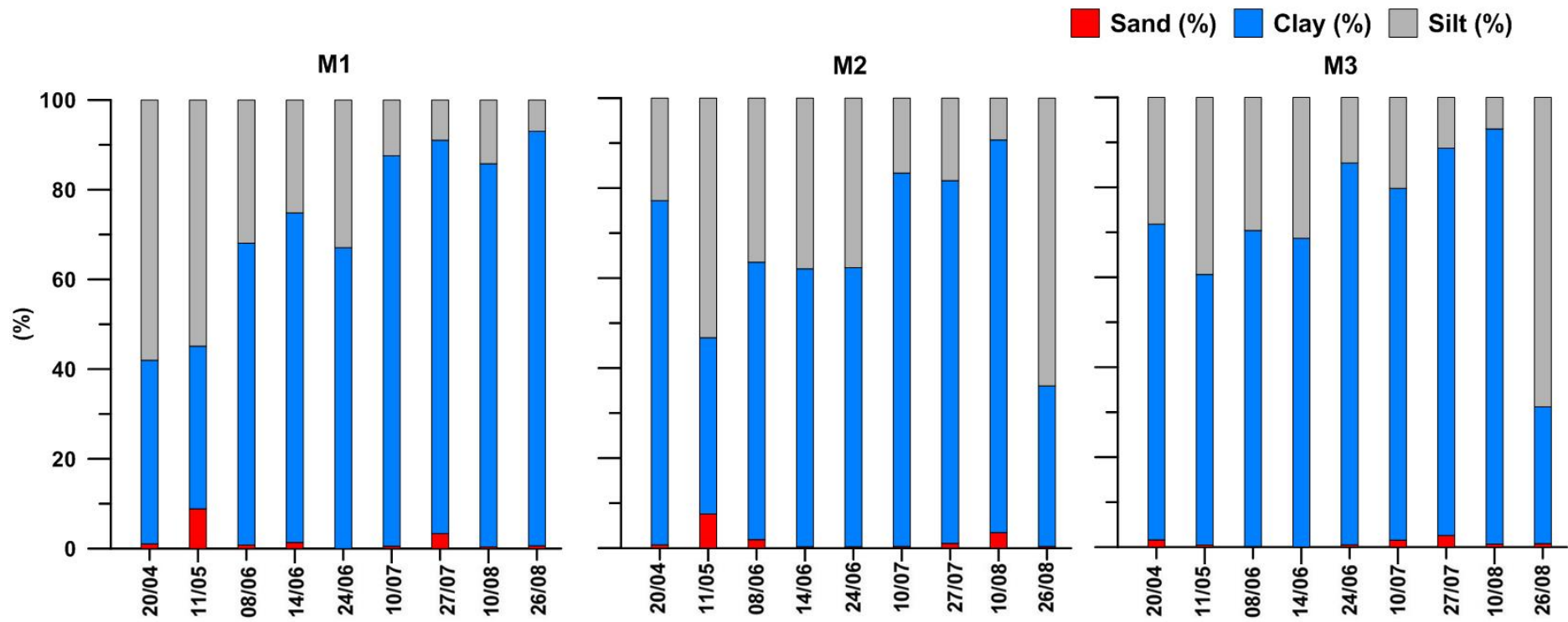


Figure 4

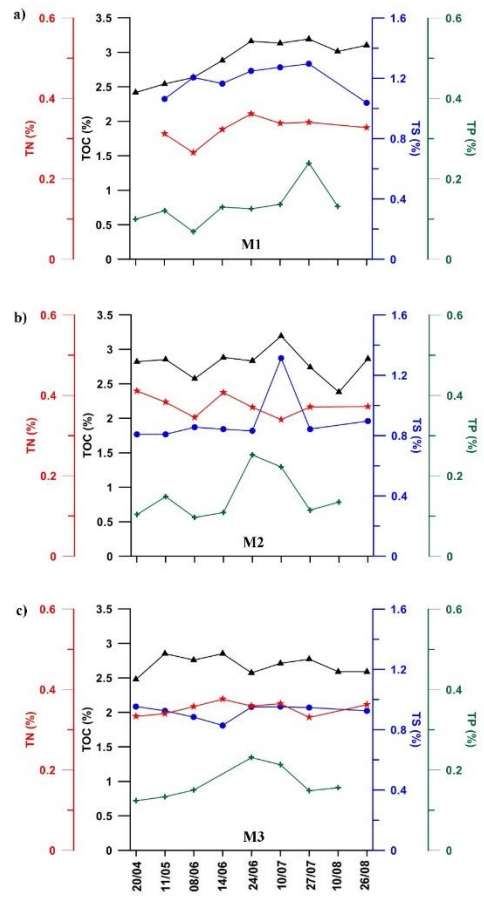


Figure 5

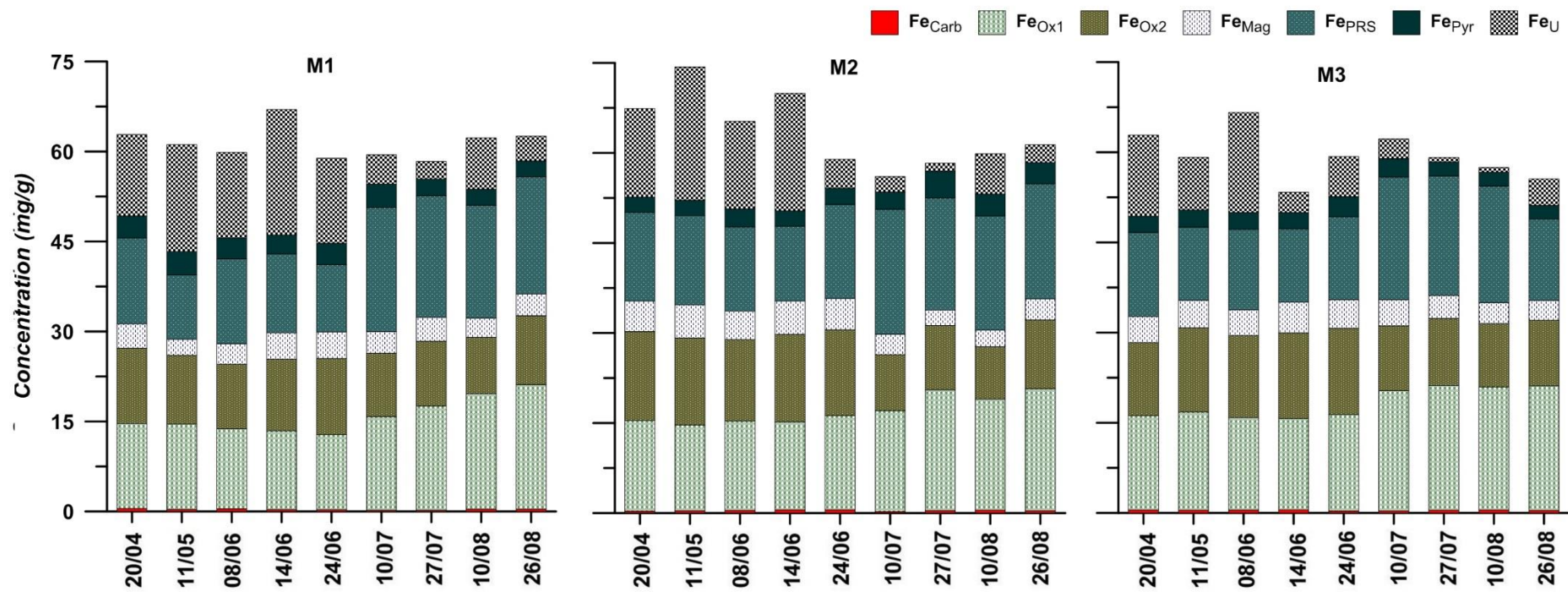


Figure 6 a

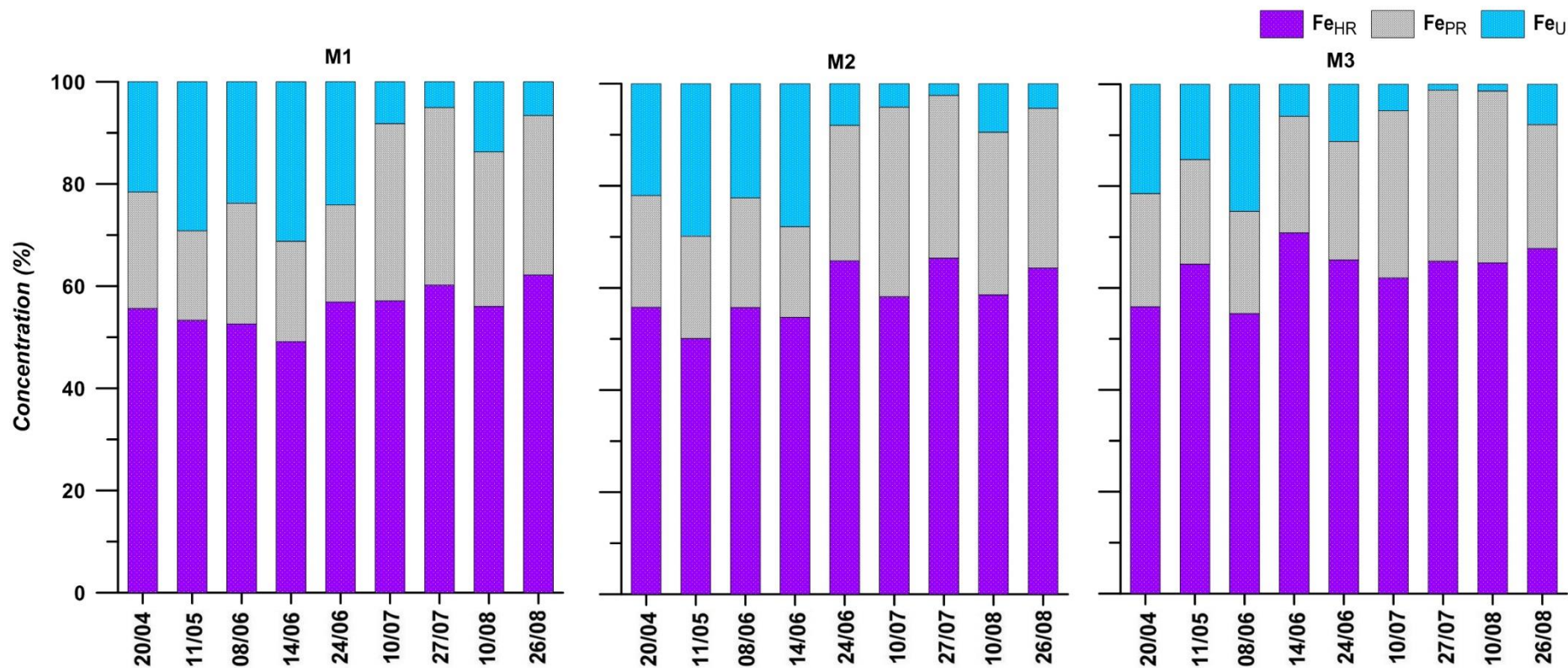


Figure 6 b

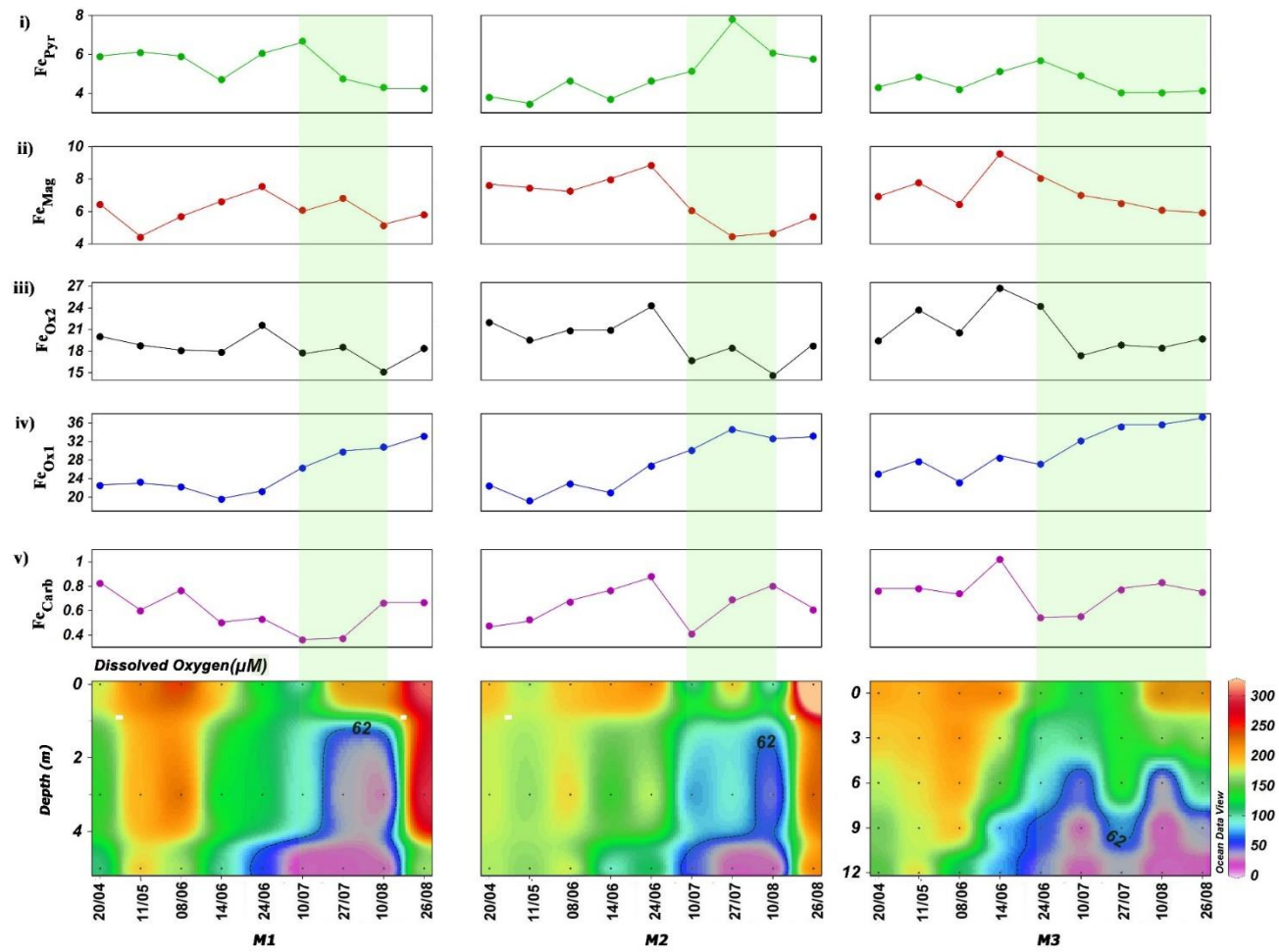


Figure 7 a

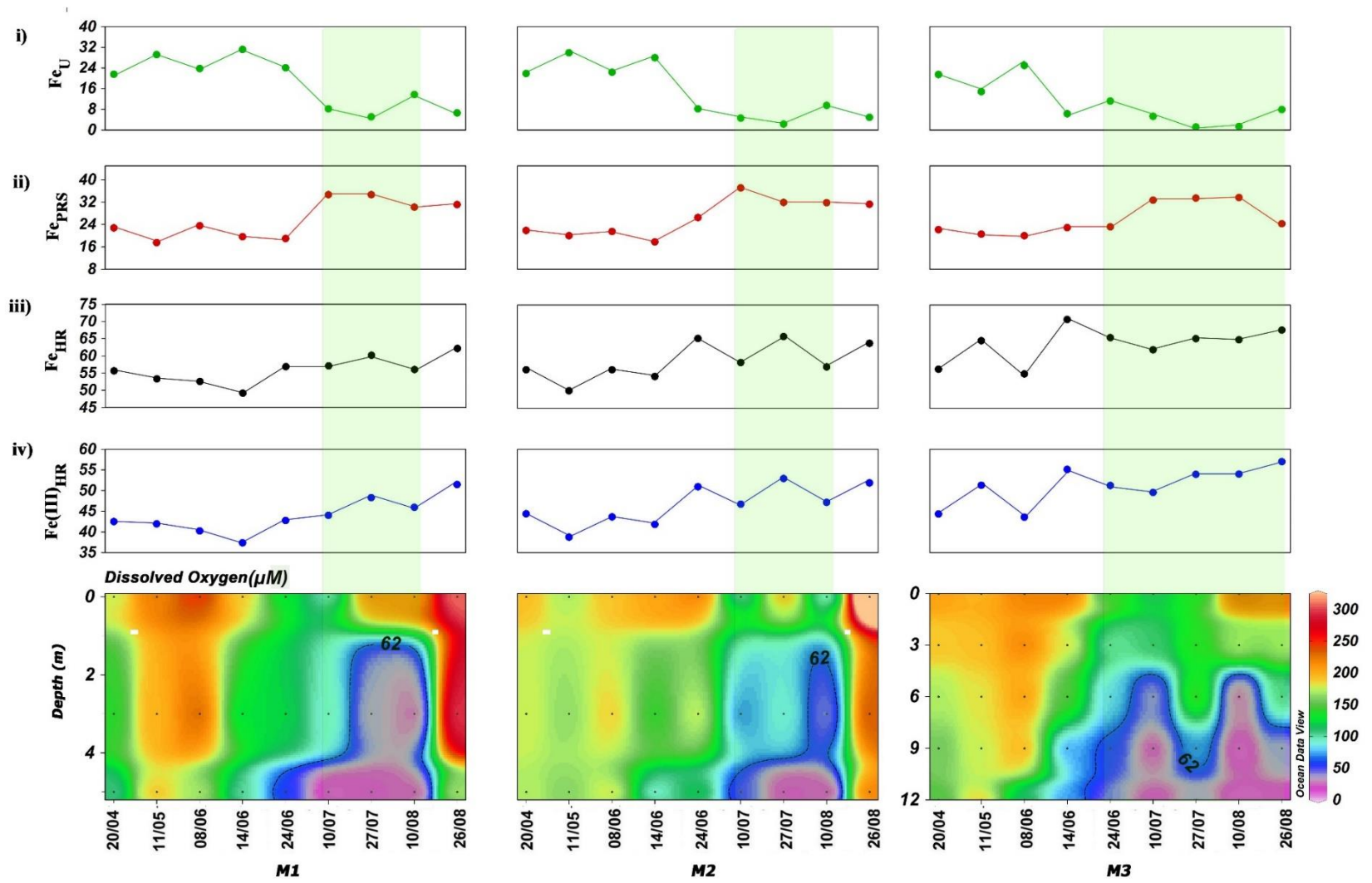


Figure 7 b